HHS Public Access

Author manuscript

Cell Rep. Author manuscript; available in PMC 2021 October 06.

Published in final edited form as:

Cell Rep. 2021 August 17; 36(7): 109561. doi:10.1016/j.celrep.2021.109561.

Rapid selection of HIV envelopes that bind to neutralizing antibody B cell lineage members with functional improbable mutations

Olivia Swanson[1], **Brianna Rhodes**[1], **Avivah Wang**[1], **Shi-Mao Xia**[1], **Robert Parks**[1], **Haiyan Chen**[1], **Aja Sanzone**[1], **Melissa Cooper**[1], **Mark K. Louder**[5], **Bob C. Lin**[5], **Nicole A. Doria-Rose**[5], **Mattia Bonsignori**[1,2], **Kevin O. Saunders**[1,3], **Kevin Wiehe**[1,2], **Barton F. Haynes**[1,2,4], **Mihai L. Azoitei**[1,2,6,*]

[1]Duke Human Vaccine Institute, Duke University, Durham, NC 27610, USA

[2]Department of Medicine, Duke University, Durham, NC 27610, USA

[3]Department of Surgery, Duke University, Durham, NC 27610, USA

[4]Department of Immunology, Duke University, Durham, NC 27610, USA

[5]Vaccine Research Center, National Institute of Allergy and Infectious Diseases, National Institutes of Health, Bethesda, MD 20814, USA

[6]Lead contact

SUMMARY

Elicitation of broadly neutralizing antibodies (bnAbs) by an HIV vaccine will involve priming the immune system to activate antibody precursors, followed by boosting immunizations to select for antibodies with functional features required for neutralization breadth. The higher the number of acquired mutations necessary for function, the more convoluted are the antibody developmental pathways. HIV bnAbs acquire a large number of somatic mutations, but not all mutations are functionally important. In this study, we identify a minimal subset of mutations sufficient for the function of the naturally occurring V3-glycan bnAb DH270.6. Using antibody library screening, candidate envelope immunogens that interact with DH270.6-like antibodies containing this set of key mutations are identified and selected *in vitro*. Our results demonstrate that less complex B cell evolutionary pathways than those naturally observed exist for the induction of HIV bnAbs by vaccination, and they establish rational approaches to identify boosting candidate immunogens.

*Correspondence: mihai.azoitei@duke.edu.

AUTHOR CONTRIBUTIONS

Conceptualization, M.L.A, O.S., K.W., and B.F.H.; methodology, M.L.A., B.F.H., K.W., K.O.S., M.B., and N.A.D.-R.; investigation, O.S., B.R., A.W., S.-M.X., R.P., H.C., A.S., M.C., M.K.L., B.C.L., and M.L.A.; writing – original draft, O.S. and M.L.A.; writing – review & editing, O.S., M.B., K.W., B.F.H., and M.L.A.; visualization, O.S. and M.L.A.; funding acquisition, B.F.H. and M.L.A.

DECLARATION OF INTERESTS

The authors declare no competing interests.

SUPPLEMENTAL INFORMATION

Supplemental information can be found online at https://doi.org/10.1016/j.celrep.2021.109561.

In brief

Swanson et. al. identify a small subset of the mutations acquired naturally by the HIV broadly neutralizing antibody DH270.6 that is sufficient for its viral neutralization function. They then develop a high-throughput method to identify candidate immunogens to elicit related lineage antibodies that contain these key mutations by vaccination.

Graphical Abstract

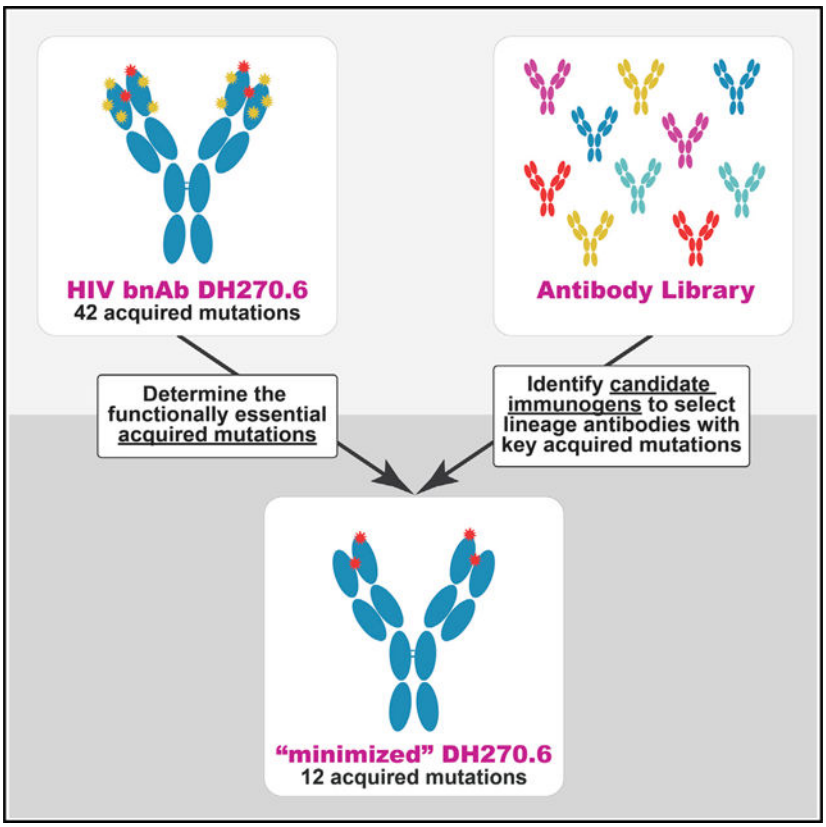

INTRODUCTION

A major goal of HIV vaccine development is to elicit broadly neutralizing antibodies (bnAbs) (Haynes et al., 2019; Kwong and Mascola, 2018). High levels of bnAbs are rarely observed upon HIV infection (Doria-Rose et al., 2010; Gray et al., 2009), although ~50% of HIV-infected individuals make detectable levels of bnAbs over time (Hraber et al., 2014). When they do occur, bnAbs typically take years to develop and their maturation follows intricate evolutionary pathways that depend on a complex interplay between viral evolution and immune adaptation (Bonsignori et al., 2017b, 2016, 2018; Doria-Rose and Landais, 2019; Gao et al., 2014; Haynes et al., 2016; Liao et al., 2013b; Wu et al., 2015).

Compared to neutralizing antibodies against other viruses such as influenza or SARS-CoV-2, HIV bnAbs acquire an unusually large number of somatic mutations, ranging from 11% to 42%, during their evolution from the unmutated common ancestor (UCA) to their

mature form (Landais and Moore, 2018; Sok et al., 2013; Wiehe et al., 2018). However, it was previously found that for two HIV bnAbs, VRC01 and BG18, only about a third of the sequence changes observed in their development are sufficient to provide neutralization breadth and potency (Jardine et al., 2016; Steichen et al., 2019). Thus, it is likely that only a subset of the naturally acquired mutations are functionally necessary for other HIV bnAbs (Georgiev et al., 2014; Wiehe et al., 2018).

Recently, it was shown that HIV bnAbs are enriched for improbable mutations acquired during affinity maturation (Shen et al., 2020; Wiehe et al., 2018). These amino acid changes are expected to happen with low frequency naturally, either because they occur in gene regions that are not typically targeted by the activation-induced cytidine deaminase (AID) or due to the number of nucleotide changes required to transform a respective UCA amino acid into the mature one (Hwang et al., 2017; Yaari et al., 2013). Notably, improbable mutations typically play a critical role in HIV bnAb function and represent developmental barriers that need to be overcome for the development of neutralization breadth (Bonsignori et al., 2017a; Shen et al., 2020). For example, in the evolution of the DH270.6 bnAb, the acquisition of an improbable glycine to arginine mutation at position 57 in the heavy chain initiates the development of heterologous neutralization breadth (Bonsignori et al., 2017a). Similarly, in the VRC34 lineage the only branch that gave rise to bnAbs acquired a rare tyrosine to proline mutation that is essential for broad neutralizing activity (Shen et al., 2020). Since improbable functional mutations represent rare events that restrict bnAb development, antibodies with such sequence changes will likely need to be explicitly selected by candidate immunogens in vaccinations.

Significant progress has been made in the design of immunogens that activate precursors of HIV bnAbs such as VRC01 and CH235.12, which target the CD4 receptor binding site and neutralize >90% of native isolates, and DH270 and BG18, which engage the glycan-V3 loop envelope (Env) region and have a global breadth of 55% and 64% respectively (Dosenovic et al., 2015; Havenar-Daughton et al., 2018; LaBranche et al., 2019; Lin et al., 2020; Saunders et al., 2019; Steichen et al., 2016, 2019; Tian et al., 2016). Immunogens targeting these antibodies have been shown to stimulate B cells displaying the respective bnAb UCAs in knockin mouse models and to promote the early development of bnAb lineages (Dosenovic et al., 2015; Escolano et al., 2016; LaBranche et al., 2019; Lin et al., 2020; Saunders et al., 2019; Steichen et al., 2019; Tian et al., 2016). However, how to further induce maturation of activated bnAb precursors to attain significant neutralization breadth remains a major challenge for HIV vaccine development. A series of boosting immunizations will likely be required following germline B cell receptor (BCR) targeting. Given the structural and functional properties of respective HIV bnAbs, immunogens may need to select for lineage B cells containing rare BCR features, such as deletions or insertions in the complementarity determining region (CDR) loops, the ability to accommodate HIV Env glycans, or the presence of functionally important improbable amino acids (Bonsignori et al., 2018; Kepler et al., 2014; Klein et al., 2013; Wiehe et al., 2018).

The V3-glycan epitope on HIV Env is targeted by diverse HIV bnAbs, such as DH270, PGT121, and BG18 (Barnes et al., 2018; Freund et al., 2017; Julien et al., 2013; Mouquet et al., 2012). Antibodies against this site have different immunogenetics, but all recognize

the conserved base of the V3 loop and one or both of the glycans present at positions 301 and 332 (Barnes et al., 2018; Mouquet et al., 2012). DH270.6 neutralized 55% of the viruses from a representative global panel of 208 pseudoviruses (half-maximal inhibitory concentration [IC_{50}] = 0.08 μg/mL) and 77.4% of those viruses containing a glycan at position 332 (Bonsignori et al., 2017a). The induction of DH270.6-like antibodies by vaccination should therefore provide significant protection against HIV infections. Unlike other bnAbs, such as PGT121 (Walker et al., 2011) and VRC01 (Wu et al., 2010), DH270.6 does not acquire any deletions or insertions in its CDR loops during development. Therefore, the elicitation of DH270.6-like bnAbs may be easier to attain in principle, and it will require the acquisition of key functional somatic mutations by putative DH270.6-like precursor antibodies.

Recently, a germline targeting immunogen was described that robustly activates DH270.6 precursors in mice when compared to an adjuvant-only control (Saunders et al., 2019). This SOSIP Env trimer, named 10.17DT, elicited DH270.6-like antibodies in DH270.6 UCA knockin mice. Isolated antibodies from animals vaccinated with 10.17DT bound the glycan moiety at position 332 and neutralized both autologous and some heterologous viruses. Importantly, some of the 10.17DT-elicited antibodies acquired improbable mutations that are essential for DH270.6 function, including heavy chain residues Arg57 and Thr98. In order to further mature the humoral responses elicited by 10.17DT, additional boosting immunizations will be required to guide antibodies toward the acquisition of somatic mutations that are essential for the neutralization breadth and potency of DH270.6 bnAb. Given the complexity of designing immunogens that direct otherwise disfavored bnAb B cell lineages to neutralization breadth, and the need to speed up immunogen design toward HIV vaccine development, a rapid iterative process is needed to rationally identify sequential immunogens capable of selecting bnAb lineage BCRs containing functional improbable mutations.

Herein, we describe a computational modeling approach to determine the functionally important somatic mutations present in HIV bnAbs and a strategy to identify and validate candidate immunogens that select antibodies with these mutations *in vitro*. We illustrate this approach by rapidly identifying the minimal functional mutations in V3-glycan bnAb DH270.6. A subset of 12 out of the 42 acquired mutations accounted for most of the DH270.6 breadth and potency. The resulting “minimized” DH270.6 antibody (DH270min) that contained these functional mutations represents a less complex HIV bnAb that can guide immunogen design and may be easier to induce by vaccination. Since a large number of the acquired mutations necessary for the function of DH270.6 were found to be improbable, antibodies containing these amino acids are predicted to occur with low frequency *in vivo*. Consequently, immunogens will have to explicitly target the enrichment of antibodies containing improbable mutations in order to induce robust protection by vaccination (Wiehe et al., 2018). To address this, we developed an immunogen selection approach that relies on high-throughput screening of antibody libraries to identify Envs that interact with DH270.6-derived antibodies through the key acquired mutations. Alternative recognition modes of DH270min that employ more probable amino acids at some of the key functional sites were also explored. This work illustrates a rational approach to identify key

functional mutations in HIV bnAbs and describes a high-throughput method to discover and validate *in vitro* immunogens that target antibody functional mutations.

RESULTS

Identification of a subset of DH270.6 acquired mutations sufficient for neutralization function

DH270.6 bnAb acquired 42 mutations during its development from UCA to the mature, broadly neutralizing form. Fourteen of these mutations ($K13N_{HC}$, $K23A_{HC}$, $I51M_{HC}$, $N54Q_{HC}$, $G57R_{HC}$, $Y60T_{HC}$, $R98T_{HC}$, $V123L_{HC}$, $S26K_{LC}$, $S27Y_{LC}$, $L48Y_{LC}$, $Q80R_{LC}$, $A93G_{LC}$, $F101C_{LC}$) are predicted to be improbable, i.e., they are expected to occur with low frequency prior to antigenic selection in the germinal center, based on computational simulations with ARMADiLLO (Wiehe et al., 2018). Structural mapping revealed that 11 mutations interact directly with the viral Env, while the other 31 are located away from the paratope (Figure 1A; Figure S1). This finding suggests that, as previously shown for other HIV bnAbs (Jardine et al., 2016; Steichen et al., 2019), not all of the DH270.6 acquired mutations may be required for broad and potent HIV neutralization. Therefore, we set to engineer a minimized DH270 antibody (DH270min) that contains only a subset of the mutations acquired by DH270.6 while recapitulating most of the bnAb function. While sequence changes located at the binding interface are likely important for function, mutations away from the paratope could also play an important role in the stability and conformation of the antibody. We used computational modeling with Rosetta (Bender et al., 2016; Das and Baker, 2008; Lauck et al., 2010; Leaver-Fay et al., 2011) to identify which of the 31 acquired mutations that do not contact the HIV Env may be important for neutralization. Diverse antibodies were built computationally on the backbone of DH270.6 that included all of the mutations located at the binding interface together with different combinations of acquired changes located away from the paratope. These different mutation subsets were manually selected because they were deemed important for DH270.6 folding and stability upon structural analysis, and they included acquired mutations located in the core of the antibody, immediately adjacent to the paratope or at the interface of the heavy and light antibody variable domains (Figure S2). For each minimized antibody candidate, acquired mutations outside the tested set were reverted to their UCA identity. The overall energies of the resulting antibodies were assessed computationally with Rosetta and compared to the energy of DH270.6. Two minimized antibodies, DH270min1 and DH270min2, that contained only 17 and 20 of the 42 mutations acquired by DH270.6, respectively, were found to have energies comparable to DH270.6 (Figure S2B) and were subsequently selected for experimental characterization. Both DH270min1 and DH270min2 included acquired mutations located at the binding interface as well as improbable mutations located immediately adjacent to the paratope (Figures 1A and 1B). DH270min2 contained additional mutations at the interface of the heavy and light chains. Three other antibodies were also tested as references: DH270min3, which contained only the DH270.6 acquired mutations located in the binding interface together with an acquired cysteine that forms a disulfide bond, as well as DH270Improb and DH270Prob that contained only the acquired improbable and probable mutations, respectively. The Rosetta energy of DH270min3 (Figure S2B) was less favorable than that of DH270.6,

DH270min1, or DH270min2, suggesting that acquired mutations located outside the paratope play important structural roles. Antibodies were expressed recombinantly, purified as immunoglobulin (Ig)Gs, and tested for neutralization on a representative panel of 15 DH270.6-sensitive HIV pseudoviruses (Figure 1C). Both DH270min1 and DH270min2 had the same neutralization breadth and potency on this panel as did wild-type (WT) DH270.6, revealing that less than half of the acquired mutations are sufficient for DH270.6 function. In contrast, DH270min3 showed significantly reduced breadth (66%) and potency (0.99 μg/mL compared to 0.09 μg/mL in DH270.6), confirming the Rosetta modeling prediction that antibody residues outside the binding interface are functionally important. Remarkably, even though there are twice as many probable mutations as improbable mutations in DH270.6, DH270Improb retained 80% of the DH270.6 breadth, while DH270Prob did not neutralize any of the viruses in the panel. DH270min1 and DH270min2 contain 10 and 7 of the total 14 improbable mutations acquired by DH270.6, respectively, showing that improbable mutations are essential for the function of this bnAb.

We next determined whether all of the 17 acquired mutations present in DH270min1 were necessary for its breadth, or whether the antibody can be further minimized by reverting additional amino acids to their UCA identity. Single mutant DH270min1 antibody variants, where each of the acquired amino acids maintained from DH270.6 were changed to the corresponding UCA residue, were expressed recombinantly and tested for neutralization as before (Figure 2A). Reversion of five of the acquired amino acids ($F32Y_{HC}$, $Q54N_{HC}$, $T60Y_{HC,}$ $K26S_{LC}$, $H32Y_{LC}$) to their DH270UCA identity had no effect on the breadth or potency of the resulting DH270min1 variants, five other mutations ($D31G_{HC}$, $M51I_{HC}$, $T55S_{HC}$, $G94S_{LC}$, $A97S_{LC}$) had a moderate effect on neutralization, while seven others ($R57G_{HC}$, $T98R_{HC}$, $Y110G_{HC,}$ $Y27S_{LC}$, $Y48L_{LC}$, $F93Y_{LC}$, $C101F_{LC}$) significantly affected the breadth and potency of the resulting DH270min1 mutants (Figure 2A). Based on these results, two other minimized antibody variants, DH270min11, which combined the 12 mutations that had some effect on antibody breadth, and DH270min12, which preserved only the 7 acquired mutations most critical for function, were developed and experimentally characterized. Compared to DH270.6 and DH270min1, these antibodies were less broad and potent on the same panel of 15 DH270.6-sensitive viruses used in the previous experiments (Figure 2A). To better assess the minimized DH270.6 variants, their neutralization was measured on a multi-clade panel of 208 viral isolates. DH270.6 was previously shown to neutralize 114 viruses from the global panel with a mean IC_{50} of 0.136 μg/mL (Bonsignori et al., 2017a). In comparison, DH270min1 neutralized 100 viruses (mean IC_{50} = 0.113 μg/mL), DH270min11 neutralized 99 viruses (mean IC_{50} = 0.135 μg/mL), and DH270min12 neutralized 68 viruses (mean IC_{50} = 0.408 μg/mL) (Figure 2B; Table S1). Therefore, DH270min11, which contained only 12 of the 42 acquired mutations, recapitulated 90% of the breadth of DH270.6, revealing that only a small subset of all DH270.6-acquired mutations is required for the development of the antibody into its broadly neutralizing form. Nine of the 12 mutations in DH270min11 ($G31D_{HC}$, $S55T_{HC}$, $G57R_{HC}$, $R98T_{HC}$, $G110Y_{HC,}$ $S27Y_{LC}$, $L48Y_{LC}$, $Y93F_{LC}$, $S97A_{LC}$) interact with the three components of the glycan-V3 epitope, the base of the V3 loop, and the glycans at positions 301 and 332, while three mutations are located away from the paratope and likely contribute to the stability and conformation of the antibody (Figure 2C). While improbable mutations make up 33% of the

total mutations acquired by DH270.6, they represent 58% (7 out of 12) of those maintained in DH270min11. Taken together, these results demonstrate that only a small fraction (28%) of the mutations acquired by DH270.6 are required for its breadth and potency. However, most of the functionally critical mutations are predicted to occur with low probability during DH270.6 development and may restrict the development of this lineage *in vivo*.

Identification of molecules that preferentially bind antibodies containing the DH270min functional mutations

DH270min11 offers a significantly shorter evolutionary pathway to elicit DH270.6-like antibodies. To identify boosting candidate immunogens that can elicit such bnAbs, we aimed to find molecules that preferentially interact with the key acquired mutations in DH270min11. We reasoned that molecules that engage residues critical for DH270.6 breadth *in vitro* may elicit antibodies with those target residues by vaccination, as was previously demonstrated for the induction of DH270.6-like precursor antibodies containing the acquired mutations $R57_{HC}$ and $T98_{HC}$ by the DH270 lineage activating immunogen 10.17DT (Saunders et al., 2019). To further mature these immune responses to breadth, boosting immunogens will be required to select additional mutations contained in DH270min11.

We previously isolated multiple HIV quasispecies that developed in subject CH848 in whom the DH270.6 V3-glycan B cell lineage arose (Bonsignori et al., 2017a). Since these Envs were isolated at different time points during the maturation of DH270.6, we reasoned that some of these molecules may be good immunogens to induce DH270.6-like Abs by vaccination. For 96 previously expressed gp120s derived from these CH848-isolated Envs (Bonsignori et al., 2017a), we measured their ELISA binding to DH270min1 and to mutated antibodies where each residue maintained from DH270.6 was reverted to its UCA identity (Figure 3; Table S2). The “selection strength” of each gp120 for a given acquired mutation present in DH270min1 was determined by calculating the ratio between its DH270min1 binding, measured as the log of the area under the curve (logAUC), and its binding to a DH270min1 antibody containing the UCA mutation at the site of interest. Therefore, the selection strength indicated the degree to which a potential immunogen engages a respective DH270min1 acquired mutation. Immunogens were considered selective for a mutation when their selection strength was greater than 2 and when they maintained strong overall binding to DH270.6 (>80% of the 10.17DT binding signal to DH270.6).

From this panel, molecules were identified that preferentially interacted with 8 of the 12 DH270.6 acquired mutations present in DH270min11, and 6 of the 7 mutations present in DH270min12 (Figure 3; Table S2). Multiple gp120s preferentially bound the antibody through the key acquired mutations $R57_{HC}$, $T98_{HC}$, $Y110_{HC}$, $Y27_{LC}$, and $Y48_{LC}$, while no gp120 selectively interacted with mutations at positions 31_{HC}, 51_{HC}, 55_{HC}, and 101_{LC}. Previously, a vaccination regimen made of sequential immunizations with Envs 10.17, 836.31, 358.06, 1432.41, and 526.02 was proposed for the elicitation of DH270.6-like antibodies (Bonsignori et al., 2017a). These immunogens were chosen based on their predicted ability to select for the $G57R_{HC}$ improbable mutation and because they have progressively longer V1 loops. These immunogens were included in this analysis and revealed that five out of the six molecules showed strong selection for at least three

mutations (Figure 3B). As a group, this immunogen panel preferentially engaged 9 out of the 12 acquired mutations in DH270min11 (Figure 3B; Table S2). However, our results indicate that more efficient sequential vaccination regimens that use a subset of these previously proposed molecules combined with newly identified ones could be developed based on our new criteria. In addition to the engagement of specific mutations, the overall affinity of an immunogen for a target antibody is also critical (Abbott et al., 2018). Both 836.31 and 1432.41 have a similar mutational selection profile, but 1432.41 has a significantly higher binding for DH270min1 (Table S2; Figure S3), which recommends its use over 836.31. While 526.02 showed strong selection for a large number of the targeted mutations, its overall affinity for DH270min1 was found to be low (Figure S3). However, our analysis identified another molecule, 526.09, that had a comparable mutational profile, but a significantly higher affinity for DH270min11 (Figure S3). The minimized DH270 can therefore be leveraged to identify molecules that preferentially interact with the key functional mutations of DH270.6.

Characterization of Envs that bind antibodies with multiple DH270min acquired mutations

In the single mutant DH270min1 antibody screen, we evaluated gp120 molecules for their ability to interact with one critical mutation at a time. However, in a vaccination scenario, immunogens will interact with BCRs clonally related to DH270.6 and that contain various amino acids at multiple sites in the binding interface. To drive DH270.6 precursors to breadth, candidate immunogens need to preferentially select from this diverse BCR repertoire the ones that contain the key acquired mutations acids identified in DH270min1. One way to assess this at the vaccine design stage is to ensure that selected immunogens preferentially interact with antibodies containing the DH270.6 amino acids over the ones present in the UCA. To predict the ability of our selected molecules to achieve this goal *in vivo*, we established an *in vitro* approach that employs high-throughput screening of single-chain variable fragment (scFv) libraries displayed on the surface of yeast (Chao et al., 2006). A library was developed that contains all of the possible scFv variants of DH270min1 with either the amino acid present in the UCA or in DH270.6 at each mutated amino acid position (Figure 4A). Therefore, this library represents a subset of the possible evolutionary paths of the DH270UCA toward DH270min1. The library was sorted by fluorescence-activated cell sorting (FACS) for binding to five different Envs: the germline targeting immunogen 10.17DT together with 1432.41, 358.06, and 526.02 identified above (Figure 4B). While gp120s were used for immunogen identification due to their availability and ease of production (Figure 3), candidate immunogens will be expressed as SOSIP Envs for immunizations and were therefore used in this format for library screening (Figure S4). The sequences of the selected scFvs bound by each Env were isolated and analyzed by next-generation sequencing. The frequency of the “mature” DH270.6 amino acids across the selected clones at each target site was compared to the frequency of that mutation in the naive library in order to determine the “enrichment levels” at a given site for the DH270.6 amino acid over the one from the UCA (Figure 4C). To validate this approach, we first compared the enrichment of amino acids selected from the scFv library by sorting with a given Env to the presence of the same mutations in antibodies elicited by vaccination with the respective molecule. The only available dataset for this analysis comes from 10.17DT, which was previously used to immunize DH270UCA knockin mice; the heavy

chain diversity of the antibody repertoire induced by vaccination was described in detail by next-generation sequencing (Saunders et al., 2019) and offers a reference dataset to compare with antibodies selected by library screening. The enrichment of a given amino acid in antibodies elicited by 10.17DT vaccination was determined by computing the ratio of the experimentally observed versus the expected frequency for that amino acid in the absence of selection (Wiehe et al., 2018). Enrichment of a given DH270.6 amino acid from the scFv library correlated well with the observed frequency of that same residue in vaccine-elicited antibodies (R^2 = 0.625 over nine positions analyzed) (Figure 4D; Figure S5). Therefore, our scFv library screening approach can describe, at least qualitatively, the ability of a given Env to elicit DH270.6-derived antibodies with target functional mutations.

Library selection and sequence analysis revealed that, taken as a group, 10.17DT, 1432.41, and 358.06 favored the mature over the UCA amino acids at 9 out of the 12 key positions in DH270min11. At three other positions, 31_{HC}, 51_{HC}, and $93_{LC,}$ the mature residues were not enriched over 10% by any of the tested Envs. The acquired mutations at position 31_{HC} and 93_{LC} are probable and expected to occur with high frequency *in vivo*, which should facilitate their selection. Indeed, significant levels of $D31_{HC}$ are observed in the repertoire of DH270UCA knockin mice vaccinated with 10.17DT (Saunders et al., 2019). Sequential immunization with 10.17DT, 1432.41, and 358.06 Envs may also present an "affinity gradient" for the selection of key amino acids at positions 55_{HC}, 57_{HC}, 98_{HC}, 110_{HC}, 94_{LC}, 97_{LC}, and 101_{LC}, based on the progressively higher enrichment levels observed for the target amino acids in the library clones selected with these three Envs. However, for the robust induction of antibodies with the full breadth of DH270.6, our results suggest that additional immunogens will likely be needed to more strongly select for key improbable mutations $M51_{HC}$, $Y27_{LC}$, and $L48_{LC}$. The scFv library was also labeled with 526.02, but only a small number (<0.1%) of clones showed binding above background, which impeded sequence analysis (data not shown). These data, corroborated by the weak binding of 526.02 to DH270min1 (Figure S3), suggest that 526.02 only interacts with DH270.6-derived antibodies that already contain most of the functional mutations required for breadth. Taken together, the scFv library screens showed that SOSIP Envs 1432.41 and 358.06 preferentially select for antibodies containing most of the acquired mutations present in DH270.6-like bnAbs.

Identification of alternative Env recognition modes by minimized DH270.6 antibodies

The significant number of functional improbable mutations in DH270.6 likely represents a barrier for the induction of similar antibodies by vaccination. While Envs can be identified that engage DH270.6-derived antibodies with these rarely occurring amino acids as shown above, it would be advantageous to discover alternative sequence variants of DH270.6-like bnAbs that may occur with higher frequency *in vivo* and may be easier to induce by vaccination. Combinations of more probable amino acids, not observed during natural evolution, may exist at the key positions in DH270min11 resulting in antibodies with alternative sequences that maintain broad neutralization.

To investigate this possibility, we aimed to identify DH270min11 variants that contain alternative amino acids at the paratope positions involved in the recognition of the V3 loop.

Three improbable acquired amino acids, including Arg57 that is critical for the development of DH270.6 breadth (Bonsignori et al., 2017b; Saunders et al., 2019), interact with the base of the V3 loop in DH20min11. A library was constructed that sampled all of the possible combinations of amino acids at these sites (55_{HC}, 57_{HC}, and 97_{LC}) together with position 51_{HC} that was judged to contribute second-shell packing interaction to the three paratope residues (Figure 5A). By sampling multiple DH270min11 improbable residues that have the same functional role, i.e., V3 loop binding, our goal was to thoroughly search for alternative Env recognition modes that rely on more probable amino acids. The resulting library of DH270min11 scFv variants was sorted in succession for binding to SOSIP Envs that were identified above (10.17DT, 358.06, and 1432.41 twice) (Figure 5B). Pseudoviruses with Envs from this panel are progressively harder to neutralize by DH270.6 and by antibodies from the same lineage that appeared earlier in the development, with 10.17DT being the easiest to neutralize (Table S3). Therefore, successive selections of the scFv library with these Envs should identify antibody sequences with increasing breadth for difficult to neutralize viruses.

Clones selected by one Env were collected, expanded, and subjected to additional sorts with the next molecules in the panel (Figure 5B). The DNA of clones bound by 10.17DT and 1432.41 was isolated and analyzed with PacBio long read sequencing technology to identify the full-length sequence of selected scFv variants. As expected, the overall sequence diversity of the isolated clones was reduced from one round of selection to the next, since fewer amino acid variants are expected to be tolerated in antibodies that bind the Envs of harder to neutralize viruses. Of note, after the last selection, the clones present with the highest frequency contained combinations of amino acids at the DH270min11 sites involved in V3 loop recognition that are not present in either the DH270.6 or its UCA (Figure 5C). Using ARMADiLLO analysis (Wiehe et al., 2018), multiple newly identified amino acids were predicted to occur with higher probability *in vivo* than those naturally present in DH270.6 (Table S4). In particular, alanine at position 57, which is expected to occur four times more frequently than the native arginine, was found to be enriched in most of the selected clones. This indicated that DH270.6-related bnAbs may exist that have diverse and more probable amino acids than do those present in the native bnAb.

To confirm this, two DH270min11 variants identified from the library, named AltMinV3_1 and AltMinV3_2, were expressed recombinantly and characterized. AltMinV3_1 contained the sequence of the most frequent clone present at the end of the selection rounds, whereas AltMinV3_2 contained more probable amino acids at all of the four V3 loop interaction positions sampled in the library. While their breadth was reduced compared to DH270min11, AltMinV3_1 and AltMinV3_2 displayed significant breadth and neutralized 10 and 7 viruses, respectively, from the panel of 15 DH270.6-sensitive isolates employed above (Figure 5D). Taken together, these results show that diverse, functionally relevant amino acid combinations can exist at key DH270.6 paratope sites, and that some of the alternative residue could occur with higher frequency *in vivo*. Therefore, multiple, more accessible pathways than the one naturally observed may exist to induce DH270.6-like antibodies by vaccination. Such pathways may be induced by the candidate immunogens identified herein, as evidenced by the ability of these SOSIPs to select for DH270.6-like

antibodies that have significant breadth and contain more probable acquired mutations in the paratope.

DISCUSSION

A major task of current HIV vaccine development efforts is to design successful vaccination regimens capable of maturing activated BCRs into bnAbs. In this study, we report a rapid strategy to identify sequential immunogen candidates that bind to bnAb lineage BCRs through the key acquired mutation required for breadth. Our results show that only a small number of acquired mutations are necessary for the development of DH270.6 V3-glycan bnAb precursors into bnAbs. Twelve amino acid changes from UCA were sufficient to recapitulate 90% of DH270.6 neutralization. While most of these mutations were located in the paratope, three of them did not directly contact HIV Env. Therefore, residues away from the binding site also modulate function, likely by affecting the antibody conformation or stability (Klein et al., 2013). Indeed, DH270min3, which contained only the acquired mutations in the paratope, displayed only 66% of the breadth of the mature bnAb. These results are in line with those reported for BG18, another HIV bnAb that targets the same glycan-V3 epitope, but uses a different binding orientation and develops from other germline genes (Barnes et al., 2018). Recently, a minimized BG18 was described that preserves 22 out of the 60 acquired mutations and recapitulates 66% of the neutralization breadth of the mature bnAb (Steichen et al., 2019). minBG18 contains only the acquired mutations located at the binding interface, while all of the amino acids located away from the paratope are reverted to their UCA identity. In comparison, by considering acquired mutations outside the binding interface in our designs, DH270min11 almost fully recapitulates the breadth of DH270.6, while maintaining a lower percentage (28%) of the total acquired mutations than does minBG18 (36%). VRC01, a bnAb that targets the CD4 binding site on Env, was the first bnAb to be minimized. minVRC01 retained 93% of the mature VRC01 breadth by preserving 24 out of the 65 acquired mutations together with a 3-aa deletion in the CDR L1 loop of the inferred UCA (Jardine et al., 2016). minVRC01 was developed by screening four different scFv libraries that sampled UCA and mature amino acids for more than 20 selection rounds (Jardine et al., 2016). Compared to this experimentally intensive approach, our strategy relied on computational and structural analysis in order to determine the residues critical for the neutralization function of DH270.6 more rapidly and at a significantly reduced cost. Amino acids that contact the HIV Env were identified from available structural data (Fera et al., 2018; Saunders et al., 2019), while residues located away from the interface critical for broad neutralizing function were determined by computational modeling. This approach identified a subset of 17 out of the 42 acquired mutations that recapitulated almost all of the DH270.6 breadth; subsequent single-site mutagenesis studies reduced this subset to 12 mutations in DH270min11. Our combined computational and experimental approach can therefore efficiently identify functionally important residues that occur during antibody development, and it should be broadly applicable to the study of other heavily mutated bnAbs.

Of the 12 acquired mutations present in the minimized DH270.6, 10 were improbable based on computational predictions that estimate the propensity of AID to mutate the antibody gene regions where they are located (Wiehe et al., 2018). HIV bnAbs are enriched for

improbable mutations, and such mutations have been shown to have important functional roles across different antibodies (Bonsignori et al., 2016; Shen et al., 2020). Forty-six percent of the acquired mutations maintained in the minVRC01 antibody and 28% of those in minBG18 are improbable. In comparison, while improbable changes constitute 33% of the acquired mutations in the DH270.6, 58% of the amino acids maintained in DH270min11 are improbable, highlighting the functional importance of these rarely occurring sequence changes for breadth development. This conclusion is further supported by our data showing that a DH270.6-derived antibody, DH270Prob, containing only the naturally acquired probable mutations had no neutralization ability (Figure 1C). Since only a small number of sequence changes, but no insertions or deletions, are required for the development of DH270.6-like bnAbs from germline precursors, these antibodies are an attractive target for elicitation by vaccination. DH270min11 is only 8% mutated from the DH270UCA, and it represents to our knowledge one of the least mutated HIV antibodies with broadly neutralizing capabilities (Simonich et al., 2016).

While DH270min11 may be easier to induce by vaccination than DH270.6, the presence of a large number of improbable mutations likely poses a significant barrier for its elicitation. However, alternative amino acids with similar functional properties that occur with higher frequency *in vivo* may exist at the sites containing improbable acquired mutations. Indeed, we found this to be the case for four DH270min11 sites that contain improbable amino acids and that are involved in interactions with the Env V3 loop. Using high-throughput library screening, non-native, more probable amino acids were found at all four sites, including position 57, which is critical for breadth development. Two tested DH270min11 antibodies containing such alternative paratope sequences maintained significant neutralization breadth, although their activity was more restricted than that of DH270min11 or DH270.6. Broader and more potent bnAbs may be isolated by subjecting the same scFv library to additional selection rounds with Envs from viruses that are more resistant to DH270.6. Nevertheless, the elicitation of a strong polyclonal response that targets the glycan-V3 epitope may provide sufficient protection, even though the individual monoclonal antibodies may not be as broad or potent as DH270.6. Our library screening experiments indicate that such bnAbs with diverse paratope sequence, containing amino acids predicted to occur frequently *in vivo*, are selected *in vitro* by the candidate immunogens identified herein. These results further highlight the potential of our proposed vaccination regimen to induce DH270.6-like bnAbs through diverse developmental pathways that are more likely to arise naturally.

Compared to previous HIV bnAb minimization studies, we leveraged our minimized DH270 antibodies to find and characterize Envs for the induction of similar antibodies by vaccination. Our approach relied on the identification of proteins that preferentially interacted with DH270.6-derived antibodies through mutations deemed essential for function. Diverse molecular properties can control the ability of candidate immunogens to contact different DH270min11 acquired mutations. The size and branching of glycans present at positions N301 and N332 can have a significant effect on antibody recognition. These glycans are variable across different Envs, and their processing is affected by the presence of neighboring glycosylation sites, like those that may exist at the tip of the V1 loop for example (Cao et al., 2017; Saunders et al., 2019; Struwe et al., 2018). In addition, sequence variation in the V3 loop can also affect molecular contacts with the acquired

mutations. Candidate immunogens were identified from a panel of gp120 molecules previously selected from the patient who gave rise to the DH270 lineage (Bonsignori et al., 2017a), based on their ability to differentially bind to minimized antibodies that either contain or lack a target mutation. Immunogens were further assessed as SOSIPs in a high-throughput fashion for their ability to select antibodies containing multiple DH270min11 acquired mutations *in vitro*. While selection of specific mutations by target immunogens in the gp120 screen correlated well with the results of the scFv library sorts, discrepancies in selection trends were observed at two sites ($S55T_{HC}$ and $F101C_{LC}$). This is probably due to the different molecular context provided by the SOSIP form of the immunogens, as well as to the different glycosylation moieties typically present in gp120 versus Env molecules at the critical 301 and 332 interaction sites. Since the SOSIP form of immunogens will be used in vaccination studies, we used the gp120 binding as a rapid way to screen a large number of molecules and the more complex scFv library screen with SOSIP Envs as a way to characterize candidate immunogens in more detail. With this approach we identified candidate immunogens 80.06 and 1432.41 that are predicted to elicit by vaccination DH270.6-like bnAbs that contain all but one of the acquired improbable mutations in DH270min11 (Figure 6). In order to more robustly select for the improbable acquired mutations $M51_{HC}$, $Y27_{LC}$, and $L48_{LC}$, additional boosting immunogens may be required. Because 80.06- and 1432.41-derived pseudo-viruses are readily neutralized by DH270min11 (Table S3), an additional “boost” may be required with a harder to bind Env that can only be recognized by antibodies with the full bnAb breadth. 526.02 Env could be such a final boosting candidate, given that it binds DH270min11 with lower affinity compared to 80.06 and 1432.41 and that its corresponding pseudo-virus is harder to neutralize by earlier antibodies that occur in the DH270.6 lineage (Table S3). Based on one available *in vivo* dataset (Saunders et al., 2019), DH270min11 residues selected from the antibody libraries by the 10.17DT immunogen correlated well with amino acids present at the same positions in antibodies elicited by 10.17DT immunizations. Nevertheless, elicitation of antibodies *in vivo* depends on many factors beyond binding affinity that are not captured in our *in vitro* characterization. For example, precursor frequency and their ability to be recruited into germinal centers by different immunizations together with the stimulation of T helper cells will be essential for the success of this vaccination regimen. (Abbott et al., 2018; Lee et al., 2020; Mesin et al., 2020). Candidate immunogens could be further validated by determining their binding affinities to inferred lineage antibodies as well as to isolated antibodies induced by vaccination with molecules that precede them in the proposed immunization schedule. Indeed, activation of target B cells has been shown to depend both on their frequency in the repertoire as well as on the affinity of the target immunogens for their BCRs (Abbott et al., 2018; Dosenovic et al., 2015; Mesin et al., 2020). The Env discovery and characterization approach presented herein is primarily meant to provide a rational way to classify and prioritize candidate immunogens for *in vivo* testing. The potential of the vaccination regimen proposed here to elicit DH270.6-like bnAbs by vaccination will be assessed in upcoming work.

HIV vaccine boosting regimens have typically been determined empirically and usually involve serial immunizations with molecules that progressively resemble the native HIV Env (Dosenovic et al., 2015; Escolano et al., 2016; Sanders et al., 2015; Steichen et al.,

2016; Tian et al., 2016). With the exception of one study that started with a later stage bnAb precursor and used sera screening and B cell repertoire analysis to inform immunogen choice (Escolano et al., 2016), such boosting regimens had limited success in maturing activated bnAb precursors (Briney et al., 2016; Dosenovic et al., 2015). Our approach aims to rationally identify and validate Envs that specifically bind to bnAb antibody lineage members bearing functional improbable mutations. Similar library platforms to the one described for DH270.6 can be developed for other HIV bnAbs, in order to identify sequential Envs that target bnAb lineages that contain rare mutations necessary for HIV neutralization breadth. In conclusion, this study describes a rational and efficient method to determine the key amino acids required for antibody function, and it establishes a generalizable approach to identify candidate Env immunogens for vaccine studies.

Limitations of study

The ability of the selected immunogens to elicit DH270.6-like antibodies needs to be demonstrated by *in vivo* vaccination studies. This study focuses on selecting antibodies with the key functional mutations of the DH270.6 bnAb. However, in a true vaccination scenario, additional strategies will be needed to disfavor other, likely immunodominant, responses that target regions outside the epitope or that engage the epitope in a way that it is not compatible with evolution to broadly neutralizing antibodies.

STAR★METHODS

RESOURCE AVAILABILITY

Lead contact—Further information and requests for resources and reagents should be directed to and will be fulfilled by the lead contact, Mihai Azoitei (mihai.azoitei@duke.edu).

Materials availability—The information and requests for resources and reagents should be directed to and will be fulfilled by the lead contact. All plasmids generated in this study are available from the lead contact.

Data and code availability

1. All data reported in this paper will be shared by the lead contact upon request.
2. This paper does not report original code.
3. Any additional information required to reanalyze the data reported in this paper is available from the lead contact upon request.

EXPERIMENTAL MODEL AND SUBJECT DETAILS

Expi293F cells (ThermoFisher) were grown in Expi293 Expression Media as per manufacturer's protocols. EBY100 yeast (ATCC; MYA-4941) were grown in SDCAA media at 30°C shaking at 220RPM and surface expression was induced with SGCAA media. NEB5α *E. coli* (NEB) were grown in Luria-Bertani (LB) broth at 37°C and shaking at 225 RPM.

METHOD DETAILS

Computational identification of functionally critical acquired mutations—

Computational design of minimally mutated DH270.6 antibodies were based on the crystal structure of the DH270.6 scFv in complex with Man9-V3 glycopeptide (PDB: 6CBP), a previously described synthetic peptide that mimics the glycan-V3 epitope on Env (Alam et al., 2017; Fera et al., 2018). Based on structural analysis, different subsets of amino acids were manually identified that were deemed important for DH270.6 stability or binding (Figure S2). All the acquired mutations located at the binding interface were included in the different subsets of mutations considered. In order to evaluate if mutations located away from the binding interface contribute to the energy of the antibody or to the conformation of the paratope, we assessed with Rosetta the energy (ref2015 scoring function (Park et al., 2016)) of different DH270.6 derived antibodies where residues deemed functionally unimportant by visual inspection were changed to their DH270UCA identity. Since the mutations evaluated in these simulations were not located in the binding site, the modeling was conducted in the absence of the epitope and only included the DH270.6 antibody (PDB: 6CBP). For each subset of acquired mutations tested, residues outside the subset were reverted to their UCA identity, and 5000 Rosetta decoys were generated for each "minimized" antibody by iterating between cycles of amino acid side chains repacking and fine backbone movement using the "backrub" protocol (Lauck et al., 2010) (Figure S2A). Antibodies with decoys that sampled Rosetta free energy levels on par with those of the mature DH270.6 were selected for experimental characterization (Figure S2).

Plasmids and DNA synthesis—

DNA for yeast display libraries was synthesized as a pooled oligo library by BioXp (CodexDNA). Genes encoding the antibody heavy and light chains were commercially synthesized and cloned into pcDNA3.1 vector (GenScript). DNA primers for sequencing and insert amplification were ordered from IDT.

Development and screening of scFv libraries on the surface of yeast

Library design and synthesis: DH270min1 sites with amino acids maintained from DH270.6 (heavy chain: G31D, Y32F, I51M, N54Q, S55T, G57R, R98T, G110Y; light chain: S26K, S27Y, Y32H, L48Y, Y60T, Y93F, A94G, S97A, F101C) were allowed to sample either the mature DH270.6 or the germline DH270UCA3 residue in an all against all fashion (library size of 1.31×10^5 scFv variants). Library DNA was synthesized as a pooled oligo library by BioXp and amplified with High Fidelity Phusion polymerase (New England Biolabs). PCR products were gel extracted (QIAGEN Gel Extraction kit) to select full length genes that were further purified (QIAGEN PCR cleanup kit) as per the manufacturer's protocol. The V3 loop library that aimed to identify alternative amino acids at the functional sites in DH270min11 maintained from DH270.6, tested all the possible amino acids combinations as follows: (heavy chain: M51, T55, R57; light chain: A97).

Library transformation into S. cerevisiae: Libraries were generated to display DH270.6 scFv variants on the surface of yeast as previously described (Benatuil et al., 2010; Chao et al., 2006). S. cerevisiae EBY100 cells were transformed by electroporation with a 3:1 ratio of 12μg scFv library DNA and 4μg pCTcon2 plasmid digested with BamHI, SalI, NheI (New England Biolabs). The typical sizes of the transformed libraries, determined by

serial dilution on selective plates, ranged from 1–5×10^7. Around 70%–90% of the sequences recovered from the transformed libraries were confirmed to contain full length, in-frame genes by Sanger sequencing. Yeast Libraries were grown in SDCAA media (Teknova) with Pen-Strep at 30C and 225 rpm.

Library screening by FACS: scFv expression on the surface of yeast was induced by culturing the libraries in SGCAA (Teknova) media at a density of 1×10^7 cellsmL for 24–36 hours. Cells were washed twice in ice cold PBSA (0.01M sodium phosphate, pH 7.4, 0.137M sodium chloride, 1g/L bovine serum albumin) and labeled with biotinylated SOSIP Envs (10.17 and 10.17DT) at a concentration of 300nM and incubated for 1hr at 4C. Cells were then washed twice with PBSA and resuspended in secondary labeling reagent 1:100 α c-*myc*:FITC (ICL) and 1:20 streptavidin:R-PE (Sigma-Aldrich) and incubated at 4C for 30 minutes. Cells were washed twice with PBSA after incubation with the fluorescently labeled probes and sorted on a BD FACS-DiVa. Double positive cells for PE and FITC were collected and expanded for one week in SDCAA media supplemented with pen-strep before successive rounds of enrichment. Sorts of the libraries with non-biotinylated SOSIPs (358.06, 1432.41, 836.31 and 0526.02) used 4-fold excess PGT151 mAb and 1:60 α-hIgG:PE (Invitrogen) pre-incubated for 60 minutes as the phycoerythrin signal. The *DH270min1 library* was screened separately for binding of SOSIPs 10.17DT, 10.17, 1432.41, 358.06, 526.02, 836.31. The *DH270min11 V3 loop library* was sorted sequentially with SOSIPS 1017.DT, 358.06, and 1432.41 twice. FACS data was analyzed with Flowjo_v10.7 software (Becton, Dickinson & Company). All clones by FACS were expanded, and their DNA was extracted (Zymo Research) for analysis by Next Generation Sequencing and Sanger sequencing analysis (Genewiz).

Sequence analysis of library clones—scFv encoding plasmids were recovered from yeast cultures by yeast miniprep with the Zymoprep yeast plasmid miniprep II kit (Zymo Research). Isolated DNA was transformed into NEB5α strain of *E. coli* (New England Biolabs) and the DNA of individual bacterial colonies was isolated (Wizard Plus SV Minipreps, Promega) and analyzed by Sanger sequencing to confirm the validity of the FACS selections. To prepare plasmids for Next Generation Sequencing, the scFv containing region from isolated plasmids was amplified by PCR using Q5 high fidelity PCR (NEB). Illumina NGS samples were prepped and run using the Illumina MiSeq v3 reagent kit following manufacturer's protocols pooling four library samples per lane. Illumina sequencing returned an average of 14.3 million reads per sample, of which an average of 13.1 million mapped to the scFv amplicon.

PacBio long read NGS was completed by Genewiz pooling 3–4 library samples per SMRT cell. Sequencing results by PacBio returned 35–47k reads per sample sequenced, of which 15–26k aligned to the scFv amplicon. Sequencing data was processed using Geneious Prime and programs developed in-house to compute the amino acid frequency and distribution.

Antibody expression and purification—Antibodies were expressed and purified as previously described (Saunders et al., 2019). Briefly, 100mL cultures of Expi293F cells at a density of 2.5×10^6 cells/mL were transiently transfected with 50μg each heavy and light chain encoding plasmids and Expifectamine (Invitrogen) per manufacturer's protocol. Five

days after transfection, cell culture media was cleared of cells by centrifugation, and the supernatant was filtered with 0.8 micron filters. Clarified supernatant was incubated with Protein A beads (Thermo Fisher) over night at 4C, washed with 20mM Tris supplemented with 350mM NaCl (pH = 7), followed by elution with a 2.5% Glacial Acetic Acid Elution Buffer and subsequent buffer exchange into 25mM Citric Acid supplemented with125mM NaCl (pH = 6). IgG expression was confirmed by reducing SDS-PAGE analysis, and quantified by measuring absorbance at 280nM (Nanodrop 2000)

Recombinant HIV Env production—SOSIP envelopes were produced recombinantly as previously described (Saunders et al., 2019). Briefly, Freestyle 293 cells were transfected with 293Fectin complexed with envelope-expressing DNA and furin-expressing plasmid DNA. After 6 days, SOSIPS were purified via PGT145 affinity chromatography with subsequent size exclusion chromatography. Trimeric HIV-1 Env fractions were pooled, snap-frozen, and stored at −80C in 10mM Tris pH 8, 500mM NaCl buffer. Expression of gp120 proteins occurred as previously described in 293F cells by transient transfection with 293Fectin (Invitrogen) and purification by metal affinity and Size Exclusion Chromatography (Alam et al., 2013; Liao et al., 2013a; Liao et al., 2006)

Pseudovirus neutralization assay—Neutralization of antibodies was measured in TZM-bl cells in a 96 or 384-well plate format assay using either a 20-virus panel comprised of viruses known to be sensitive to DH270.6, or on a 208 Env-pseudovirus panel representative of the major genetic subtypes of circulating virus (Bonsignori et al., 2017a; Bonsignori et al., 2016). Signal was calculated as a reduction in luminescence compared to control wells and reported as IC_{50} in μg/mL. Neutralization data displayed in Figures 1, 2, and 5 is representative of at least 2 independent measurements.

ELISA assay—Direct-binding ELISAs were performed as described on 96 gp120 molecules isolated previously (Bonsignori et al., 2017a; Bonsignori et al., 2016). Sequences for the 96 gp120s can be located by using the Los Alamos HIV Sequence Compendium (https://www.hiv.lanl.gov) and searching by the patient code CH848 (Foley et al., 2018). Briefly, ELISAs were carried out as follows: 384-well plates were blocked overnight at 4C. Starting concentrations of 100ug/mL purified antibody were serially diluted 3-fold and incubated at room temperature for 1 hour. 1:15,000 HRP- conjugated hIgG in assay diluent was added to plates, incubated for one hour, and developed using TMB substrate. Plates were read at 450nm on a SpectraMax 384 PLUS reader (Molecular Devices).

QUANTIFICATION AND STATISTICAL ANALYSIS

Statistical details of experiments can be found in the Methods and Results. ELISA log Area Under the Curve (logAUC) was calculated with SoftMax Pro (v 5.3).

Supplementary Material

Refer to Web version on PubMed Central for supplementary material.

ACKNOWLEDGMENTS

We thank J. Baalwa, D. Ellenberger, F. Gao, B. Hahn, K. Hong, J. Kim, F. McCutchan, D. Montefiori, L. Morris, E. Sanders-Buell, G. Shaw, R. Swanstrom, M. Thomson, S. Tovanabutra, C. Williamson, and L. Zhang for contributing the HIV-1 envelope plasmids used in the 208-strain panel. We thank K. McKee, C. Moore, S. O'Dell, G. Padilla, S.D. Schmidt, C. Whittaker, and A.B. McDermott for assistance with neutralization assessments on the 208-strain panel. Library prep and Illumina sequencing were provided by the Viral Genetics and Analysis Core Facility in the Duke Human Vaccine Institute. Fluorescence-activated cell sorting of yeast display libraries was performed at the Flow Cytometry Shared Resource (FCSR) in the Duke Cancer Institute. This work was supported by NIH.NIAID/Division of AIDS UM1 grant AI144371 for the Consortium for HIV/AIDS Vaccine Development (to B.F.H.) and funding from the Duke Translational Health Initiative (to M.L.A.).

REFERENCES

Abbott RK, Lee JH, Menis S, Skog P, Rossi M, Ota T, Kulp DW, Bhullar D, Kalyuzhniy O, Havenar-Daughton C, et al. (2018). Precursor frequency and affinity determine B cell competitive fitness in germinal centers, tested with germline-targeting HIV vaccine immunogens. Immunity 48, 133–146.e6. [PubMed: 29287996]

Alam SM, Liao H-X, Tomaras GD, Bonsignori M, Tsao C-Y, Hwang K-K, Chen H, Lloyd KE, Bowman C, Sutherland L, et al. (2013). Antigenicity and immunogenicity of RV144 vaccine AIDSVAX clade E envelope immunogen is enhanced by a gp120 N-terminal deletion. J. Virol. 87, 1554–1568. [PubMed: 23175357]

Alam SM, Aussedat B, Vohra Y, Meyerhoff RR, Cale EM, Walkowicz WE, Radakovich NA, Anasti K, Armand L, Parks R, et al. (2017). Mimicry of an HIV broadly neutralizing antibody epitope with a synthetic glycopeptide. Sci. Transl. Med. 9, eaai7521. [PubMed: 28298421]

Barnes CO, Gristick HB, Freund NT, Escolano A, Lyubimov AY, Hartweger H, West AP Jr., Cohen AE, Nussenzweig MC, and Bjorkman PJ (2018). Structural characterization of a highly-potent V3-glycan broadly neutralizing antibody bound to natively-glycosylated HIV-1 envelope. Nat. Commun. 9, 1251. [PubMed: 29593217]

Benatuil L, Perez JM, Belk J, and Hsieh CM (2010). An improved yeast transformation method for the generation of very large human antibody libraries. Protein Eng. Des. Sel. 23, 155–159. [PubMed: 20130105]

Bender BJ, Cisneros A 3rd, Duran AM, Finn JA, Fu D, Lokits AD, Mueller BK, Sangha AK, Sauer MF, Sevy AM, et al. (2016). Protocols for molecular modeling with Rosetta3 and RosettaScripts. Biochemistry 55, 4748–4763. [PubMed: 27490953]

Bonsignori M, Zhou T, Sheng Z, Chen L, Gao F, Joyce MG, Ozorowski G, Chuang G-Y, Schramm CA, Wiehe K, et al. ; NISC Comparative Sequencing Program (2016). Maturation pathway from germline to broad HIV-1 neutralizer of a CD4-mimic antibody. Cell 165, 449–463. [PubMed: 26949186]

Bonsignori M, Kreider EF, Fera D, Meyerhoff RR, Bradley T, Wiehe K, Alam SM, Aussedat B, Walkowicz WE, Hwang KK, et al. (2017a). Staged induction of HIV-1 glycan-dependent broadly neutralizing antibodies. Sci. Transl. Med. 9, eaai7514. [PubMed: 28298420]

Bonsignori M, Liao HX, Gao F, Williams WB, Alam SM, Montefiori DC, and Haynes BF (2017b). Antibody-virus co-evolution in HIV infection: Paths for HIV vaccine development. Immunol. Rev. 275, 145–160. [PubMed: 28133802]

Bonsignori M, Scott E, Wiehe K, Easterhoff D, Alam SM, Hwang KK, Cooper M, Xia SM, Zhang R, Montefiori DC, et al. (2018). Inference of the HIV-1 VRC01 antibody lineage unmutated common ancestor reveals alternative pathways to overcome a key glycan barrier. Immunity 49, 1162–1174.e8. [PubMed: 30552024]

Briney B, Sok D, Jardine JG, Kulp DW, Skog P, Menis S, Jacak R, Kalyuzhniy O, de Val N, Sesterhenn F, et al. (2016). Tailored immunogens direct affinity maturation toward HIV neutralizing antibodies. Cell 166, 1459–1470.e11. [PubMed: 27610570]

Cao L, Diedrich JK, Kulp DW, Pauthner M, He L, Park SR, Sok D, Su CY, Delahunty CM, Menis S, et al. (2017). Global site-specific N-glycosylation analysis of HIV envelope glycoprotein. Nat. Commun. 8, 14954. [PubMed: 28348411]

Chao G, Lau WL, Hackel BJ, Sazinsky SL, Lippow SM, and Wittrup KD (2006). Isolating and engineering human antibodies using yeast surface display. Nat. Protoc. 1, 755–768. [PubMed: 17406305]

Crooks GE, Hon G, Chandonia J-M, and Brenner S (2004). WebLogo: a sequence logo generator. Genome Research 14, 1188–1190. 10.1101/gr.849004. [PubMed: 15173120]

Das R, and Baker D (2008). Macromolecular modeling with Rosetta. Annu. Rev. Biochem. 77, 363–382. [PubMed: 18410248]

Doria-Rose NA, and Landais E (2019). Coevolution of HIV-1 and broadly neutralizing antibodies. Curr. Opin. HIV AIDS 14, 286–293. [PubMed: 30994504]

Doria-Rose NA, Klein RM, Daniels MG, O'Dell S, Nason M, Lapedes A, Bhattacharya T, Migueles SA, Wyatt RT, Korber BT, et al. (2010). Breadth of human immunodeficiency virus-specific neutralizing activity in sera: Clustering analysis and association with clinical variables. J. Virol. 84, 1631–1636. [PubMed: 19923174]

Dosenovic P, von Boehmer L, Escolano A, Jardine J, Freund NT, Gitlin AD, McGuire AT, Kulp DW, Oliveira T, Scharf L, et al. (2015). Immunization for HIV-1 broadly neutralizing antibodies in human Ig knockin mice. Cell 161, 1505–1515. [PubMed: 26091035]

Escolano A, Steichen JM, Dosenovic P, Kulp DW, Golijanin J, Sok D, Freund NT, Gitlin AD, Oliveira T, Araki T, et al. (2016). Sequential immunization elicits broadly neutralizing anti-HIV-1 antibodies in Ig knockin mice. Cell 166, 1445–1458.e12. [PubMed: 27610569]

Fera D, Lee MS, Wiehe K, Meyerhoff RR, Piai A, Bonsignori M, Aussedat B, Walkowicz WE, Ton T, Zhou JO, et al. (2018). HIV envelope V3 region mimic embodies key features of a broadly neutralizing antibody lineage epitope. Nat. Commun. 9, 1111. [PubMed: 29549260]

Foley BLT, Apetrei C, Hahn B, Mizrachi I, Mullins J, Rambaut A, Wolinsky S, and Korber B (2018). HIV Sequence Compendium 2018 (Theoretical Biology and Biophysics Group, Los Alamos National Laboratory). https://permalink.lanl.gov/object/tr?what=info:lanl-repo/lareport/LA-UR-18-25673.

Freund NT, Wang H, Scharf L, Nogueira L, Horwitz JA, Bar-On Y, Golijanin J, Sievers SA, Sok D, Cai H, et al. (2017). Coexistence of potent HIV-1 broadly neutralizing antibodies and antibody-sensitive viruses in a viremic controller. Sci. Transl. Med. 9, eaal2144. [PubMed: 28100831]

Gao F, Bonsignori M, Liao HX, Kumar A, Xia SM, Lu X, Cai F, Hwang KK, Song H, Zhou T, et al. (2014). Cooperation of B cell lineages in induction of HIV-1-broadly neutralizing antibodies. Cell 158, 481–491. [PubMed: 25065977]

Georgiev IS, Rudicell RS, Saunders KO, Shi W, Kirys T, McKee K, O'Dell S, Chuang G-Y, Yang Z-Y, Ofek G, et al. (2014). Antibodies VRC01 and 10E8 neutralize HIV-1 with high breadth and potency even with Ig-framework regions substantially reverted to germline. J. Immunol. 192, 1100–1106. [PubMed: 24391217]

Gray ES, Taylor N, Wycuff D, Moore PL, Tomaras GD, Wibmer CK, Puren A, DeCamp A, Gilbert PB, Wood B, et al. (2009). Antibody specificities associated with neutralization breadth in plasma from human immunodeficiency virus type 1 subtype C-infected blood donors. J. Virol. 83, 8925–8937. [PubMed: 19553335]

Havenar-Daughton C, Sarkar A, Kulp DW, Toy L, Hu X, Deresa I, Kalyuzhniy O, Kaushik K, Upadhyay AA, Menis S, et al. (2018). The human naive B cell repertoire contains distinct subclasses for a germline-targeting HIV-1 vaccine immunogen. Sci. Transl. Med. 10, eaat0381. [PubMed: 29973404]

Haynes BF, Shaw GM, Korber B, Kelsoe G, Sodroski J, Hahn BH, Borrow P, and McMichael AJ (2016). HIV-host interactions: Implications for vaccine design. Cell Host Microbe 19, 292–303. [PubMed: 26922989]

Haynes BF, Burton DR, and Mascola JR (2019). Multiple roles for HIV broadly neutralizing antibodies. Sci. Transl. Med. 11, eaaz2686. [PubMed: 31666399]

Hraber P, Seaman MS, Bailer RT, Mascola JR, Montefiori DC, and Korber BT (2014). Prevalence of broadly neutralizing antibody responses during chronic HIV-1 infection. AIDS 28, 163–169. [PubMed: 24361678]

Hwang JK, Wang C, Du Z, Meyers RM, Kepler TB, Neuberg D, Kwong PD, Mascola JR, Joyce MG, Bonsignori M, et al. (2017). Sequence intrinsic somatic mutation mechanisms contribute to affinity

maturation of VRC01-class HIV-1 broadly neutralizing antibodies. Proc. Natl. Acad. Sci. USA 114, 8614–8619. [PubMed: 28747530]

Jardine JG, Sok D, Julien JP, Briney B, Sarkar A, Liang CH, Scherer EA, Henry Dunand CJ, Adachi Y, Diwanji D, et al. (2016). Minimally mutated HIV-1 broadly neutralizing antibodies to guide reductionist vaccine design. PLoS Pathog. 12, e1005815. [PubMed: 27560183]

Julien J-P, Sok D, Khayat R, Lee JH, Doores KJ, Walker LM, Ramos A, Diwanji DC, Pejchal R, Cupo A, et al. (2013). Broadly neutralizing antibody PGT121 allosterically modulates CD4 binding via recognition of the HIV-1 gp120 V3 base and multiple surrounding glycans. PLoS Pathog. 9, e1003342. [PubMed: 23658524]

Kepler TB, Liao H-X, Alam SM, Bhaskarabhatla R, Zhang R, Yandava C, Stewart S, Anasti K, Kelsoe G, Parks R, et al. (2014). Immunoglobulin gene insertions and deletions in the affinity maturation of HIV-1 broadly reactive neutralizing antibodies. Cell Host Microbe 16, 304–313. [PubMed: 25211073]

Klein F, Diskin R, Scheid JF, Gaebler C, Mouquet H, Georgiev IS, Pancera M, Zhou T, Incesu RB, Fu BZ, et al. (2013). Somatic mutations of the immunoglobulin framework are generally required for broad and potent HIV-1 neutralization. Cell 153, 126–138. [PubMed: 23540694]

Krissinel E, and Henrick K (2007). Inference of macromolecular assemblies from crystalline state. Journal of Molecular Biology. 10.1016/j.jmb.2007.05.022.

Kwong PD, and Mascola JR (2018). HIV-1 vaccines based on antibody identification, B cell ontogeny, and epitope structure. Immunity 48, 855–871. [PubMed: 29768174]

LaBranche CC, Henderson R, Hsu A, Behrens S, Chen X, Zhou T, Wiehe K, Saunders KO, Alam SM, Bonsignori M, et al. (2019). Neutralization-guided design of HIV-1 envelope trimers with high affinity for the unmutated common ancestor of CH235 lineage CD4bs broadly neutralizing antibodies. PLoS Pathog. 15, e1008026. [PubMed: 31527908]

Landais E, and Moore PL (2018). Development of broadly neutralizing antibodies in HIV-1 infected elite neutralizers. Retrovirology 15, 61. [PubMed: 30185183]

Lauck F, Smith CA, Friedland GF, Humphris EL, and Kortemme T (2010). RosettaBackrub—A web server for flexible backbone protein structure modeling and design. Nucleic Acids Res. 38, W569–75. [PubMed: 20462859]

Leaver-Fay A, Tyka M, Lewis SM, Lange OF, Thompson J, Jacak R, Kaufman K, Renfrew PD, Smith CA, Sheffler W, et al. (2011). ROSETTA3: An object-oriented software suite for the simulation and design of macromolecules. Methods Enzymol. 487, 545–574. [PubMed: 21187238]

Lee JH, Nakao C, Moyer TJ, Irvine DJ, Schief WR, and Crotty S (2020). Exploration of roles of CD4 T cell help in recruitment of rare B cells to germinal centers. J. Immunol. 204 (1 Suppl), 167.165.

Liao H-X, Sutherland LL, Xia S-M, Brock ME, Scearce RM, Vanleeuwen S, Alam SM, McAdams M, Weaver EA, Camacho Z, et al. (2006). A group M consensus envelope glycoprotein induces antibodies that neutralize subsets of subtype B and C HIV-1 primary viruses. Virology 353, 268–282. [PubMed: 17039602]

Liao H-X, Bonsignori M, Alam SM, McLellan JS, Tomaras GD, Moody MA, Kozink DM, Hwang KK, Chen X, Tsao CY, et al. (2013a). Vaccine induction of antibodies against a structurally heterogeneous site of immune pressure within HIV-1 envelope protein variable regions 1 and 2. Immunity 38, 176–186. [PubMed: 23313589]

Liao HX, Lynch R, Zhou T, Gao F, Alam SM, Boyd SD, Fire AZ, Roskin KM, Schramm CA, Zhang Z, et al. ; NISC Comparative Sequencing Program (2013b). Co-evolution of a broadly neutralizing HIV-1 antibody and founder virus. Nature 496, 469–476. [PubMed: 23552890]

Lin YR, Parks KR, Weidle C, Naidu AS, Khechaduri A, Riker AO, Takushi B, Chun JH, Borst AJ, Veesler D, et al. (2020). HIV-1 VRC01 germline-targeting immunogens select distinct epitope-specific B cell receptors. Immunity 53, 840–851.e6. [PubMed: 33053332]

Mesin L, Schiepers A, Ersching J, Barbulescu A, Cavazzoni CB, Angelini A, Okada T, Kurosaki T, and Victora GD (2020). Restricted clonality and limited germinal center reentry characterize memory B cell reactivation by boosting. Cell 180, 92–106.e11. [PubMed: 31866068]

Mouquet H, Scharf L, Euler Z, Liu Y, Eden C, Scheid JF, Halper-Stromberg A, Gnanapragasam PNP, Spencer DIR, Seaman MS, et al. (2012). Complex-type N-glycan recognition by potent broadly neutralizing HIV antibodies. Proc. Natl. Acad. Sci. USA 109, E3268–E3277. [PubMed: 23115339]

Park H, Bradley P, Greisen P Jr., Liu Y, Mulligan VK, Kim DE, Baker D, and DiMaio F (2016). Simultaneous optimization of biomolecular energy functions on features from small molecules and macromolecules. J. Chem. Theory Comput. 12, 6201–6212. [PubMed: 27766851]

Sanders RW, van Gils MJ, Derking R, Sok D, Ketas TJ, Burger JA, Ozorowski G, Cupo A, Simonich C, Goo L, et al. (2015). HIV-1 neutralizing antibodies induced by native-like envelope trimers. Science 349, aac4223. [PubMed: 26089353]

Saunders KO, Wiehe K, Tian M, Acharya P, Bradley T, Alam SM, Go EP, Scearce R, Sutherland L, Henderson R, et al. (2019). Targeted selection of HIV-specific antibody mutations by engineering B cell maturation. Science 366, eaay7199. [PubMed: 31806786]

Shen CH, DeKosky BJ, Guo Y, Xu K, Gu Y, Kilam D, Ko SH, Kong R, Liu K, Louder MK, et al. (2020). VRC34-antibody lineage development reveals how a required rare mutation shapes the maturation of a broad HIV-neutralizing lineage. Cell Host Microbe 27, 531–543.e6. [PubMed: 32130953]

Simonich CA, Williams KL, Verkerke HP, Williams JA, Nduati R, Lee KK, and Overbaugh J (2016). HIV-1 neutralizing antibodies with limited hypermutation from an infant. Cell 166, 77–87. [PubMed: 27345369]

Sok D, Laserson U, Laserson J, Liu Y, Vigneault F, Julien JP, Briney B, Ramos A, Saye KF, Le K, et al. (2013). The effects of somatic hypermutation on neutralization and binding in the PGT121 family of broadly neutralizing HIV antibodies. PLoS Pathog. 9, e1003754. [PubMed: 24278016]

Steichen JM, Kulp DW, Tokatlian T, Escolano A, Dosenovic P, Stanfield RL, McCoy LE, Ozorowski G, Hu X, Kalyuzhniy O, et al. (2016). HIV vaccine design to target germline precursors of glycan-dependent broadly neutralizing antibodies. Immunity 45, 483–496. [PubMed: 27617678]

Steichen JM, Lin YC, Havenar-Daughton C, Pecetta S, Ozorowski G, Willis JR, Toy L, Sok D, Liguori A, Kratochvil S, et al. (2019). A generalized HIV vaccine design strategy for priming of broadly neutralizing antibody responses. Science 366, eaax4380. [PubMed: 31672916]

Struwe WB, Chertova E, Allen JD, Seabright GE, Watanabe Y, Harvey DJ, Medina-Ramirez M, Roser JD, Smith R, Westcott D, et al. (2018). Site-specific glycosylation of virion-derived HIV-1 Env is mimicked by a soluble trimeric immunogen. Cell Rep. 24, 1958–1966.e5. [PubMed: 30134158]

Tian M, Cheng C, Chen X, Duan H, Cheng H-L, Dao M, Sheng Z, Kimble M, Wang L, Lin S, et al. (2016). Induction of HIV neutralizing antibody lineages in mice with diverse precursor repertoires. Cell 166, 1471–1484.e18. [PubMed: 27610571]

Walker LM, Huber M, Doores KJ, Falkowska E, Pejchal R, Julien JP, Wang SK, Ramos A, Chan-Hui PY, Moyle M, et al. ; Protocol G Principal Investigators (2011). Broad neutralization coverage of HIV by multiple highly potent antibodies. Nature 477, 466–470. [PubMed: 21849977]

Wiehe K, Bradley T, Meyerhoff RR, Hart C, Williams WB, Easterhoff D, Faison WJ, Kepler TB, Saunders KO, Alam SM, et al. (2018). Functional relevance of improbable antibody mutations for HIV broadly neutralizing antibody development. Cell Host Microbe 23, 759–765.e6. [PubMed: 29861171]

Wu X, Yang ZY, Li Y, Hogerkorp CM, Schief WR, Seaman MS, Zhou T, Schmidt SD, Wu L, Xu L, et al. (2010). Rational design of envelope identifies broadly neutralizing human monoclonal antibodies to HIV-1. Science 329, 856–861. [PubMed: 20616233]

Wu X, Zhang Z, Schramm CA, Joyce MG, Kwon YD, Zhou T, Sheng Z, Zhang B, O'Dell S, McKee K, et al. ; NISC Comparative Sequencing Program (2015). Maturation and diversity of the VRC01-antibody lineage over 15 years of chronic HIV-1 infection. Cell 161, 470–485. [PubMed: 25865483]

Yaari G, Vander Heiden JA, Uduman M, Gadala-Maria D, Gupta N, Stern JNH, O'Connor KC, Hafler DA, Laserson U, Vigneault F, and Kleinstein SH (2013). Models of somatic hypermutation targeting and substitution based on synonymous mutations from high-throughput immunoglobulin sequencing data. Front. Immunol. 4, 358, 358.

Highlights

- Few naturally acquired mutations are required for the function of HIV bnAb DH270.6
- Acquired improbable mutations are critical for neutralization
- Immunogens to elicit lineage Abs containing key DH270.6 mutations are identified
- More probable evolution pathways to induce DH270.6-like bnAbs likely exist

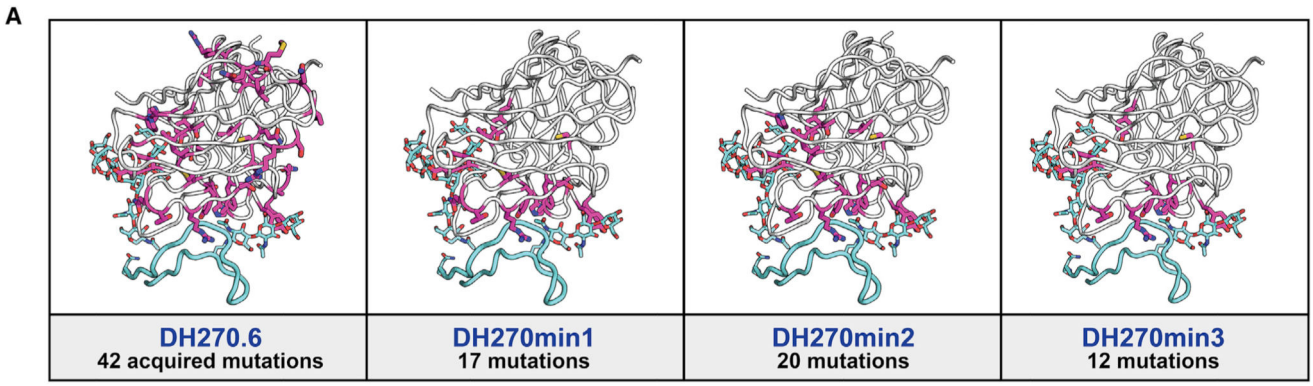

B

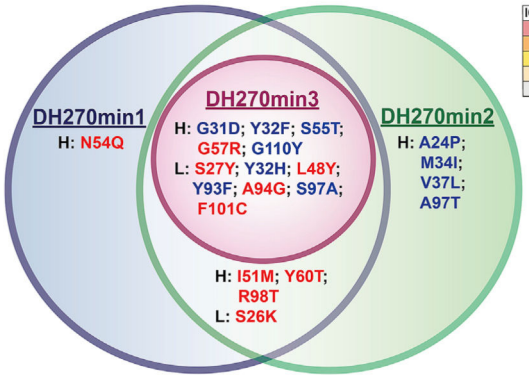

C

IC50 ug/ml
< 0.1
0.1 to 1
1 to 10
10 to 50
>50

	DH270.6	min1	min2	min3	Improb	Prob
92RW020	0.021	<0.023	<0.023	0.025	<0.023	>50
ZM55F.PB28a	0.03	<0.023	<0.023	0.585	0.041	>50
6101.10	0.04	<0.023	<0.023	0.12	<0.023	>50
JRFL	0.04	<0.023	<0.023	19.651	0.034	>50
ZM106F.PB9	0.05	<0.023	<0.023	0.096	<0.023	>50
DU156.12	0.07	0.068	0.078	0.989	0.158	>50
TRO.11	0.06	<0.023	<0.023	0.635	0.48	>50
DJ263.B	0.08	0.036	<0.023	10.882	1.43	>50
CAAN5342.a2	0.03	<0.023	<0.023	11.024	1.652	>50
DU422.1	0.19	0.192	0.202	3.776	0.315	>50
PVO.4	0.14	0.12	0.093	>50	34.477	>50
CNE58	0.28	0.166	0.074	>50	29.779	>50
TRJO4551.58	0.194	<0.023	<0.023	>50	>50	>50
DU172.17	0.27	0.258	0.303	>50	>50	>50
57128.vrc15	2	7.925	7.631	>50	>50	>50
Breadth	100.0%	100.0%	100.0%	66.7%	80.0%	0.0%
Potency	0.09	0.06	0.06	0.99	0.32	N/A
# AA Muts	45	17	20	12	14	28

Figure 1. Design of first-generation minimized DH270.6 antibodies

(A) Structural mapping of DH270.6 somatic mutations maintained in different DH270min variants. Mutations (magenta, sticks) were mapped on the structure of DH270.6 scFv (gray) in complex with an HIV Env-derived V3-loop glycopeptide (cyan) (“PDB: 6cbp”). Glycans at positions N301 and N332 are shown in sticks.

(B) Venn diagram of the acquired mutations present in the DH270min antibodies colored by their predicted *in vivo* probability (high is shown blue; low is shown in red).

(C) Neutralization breadth and potency of DH270.6, DH270min antibodies, and DH270.6 variants that contain only the “probable” (DH270Prob) or “improbable” mutations (DH270Improb) on a panel of DH270.6-sensitive pseudoviruses. # AA Muts, the number of DH270.6-acquired mutations maintained in the respective antibodies.

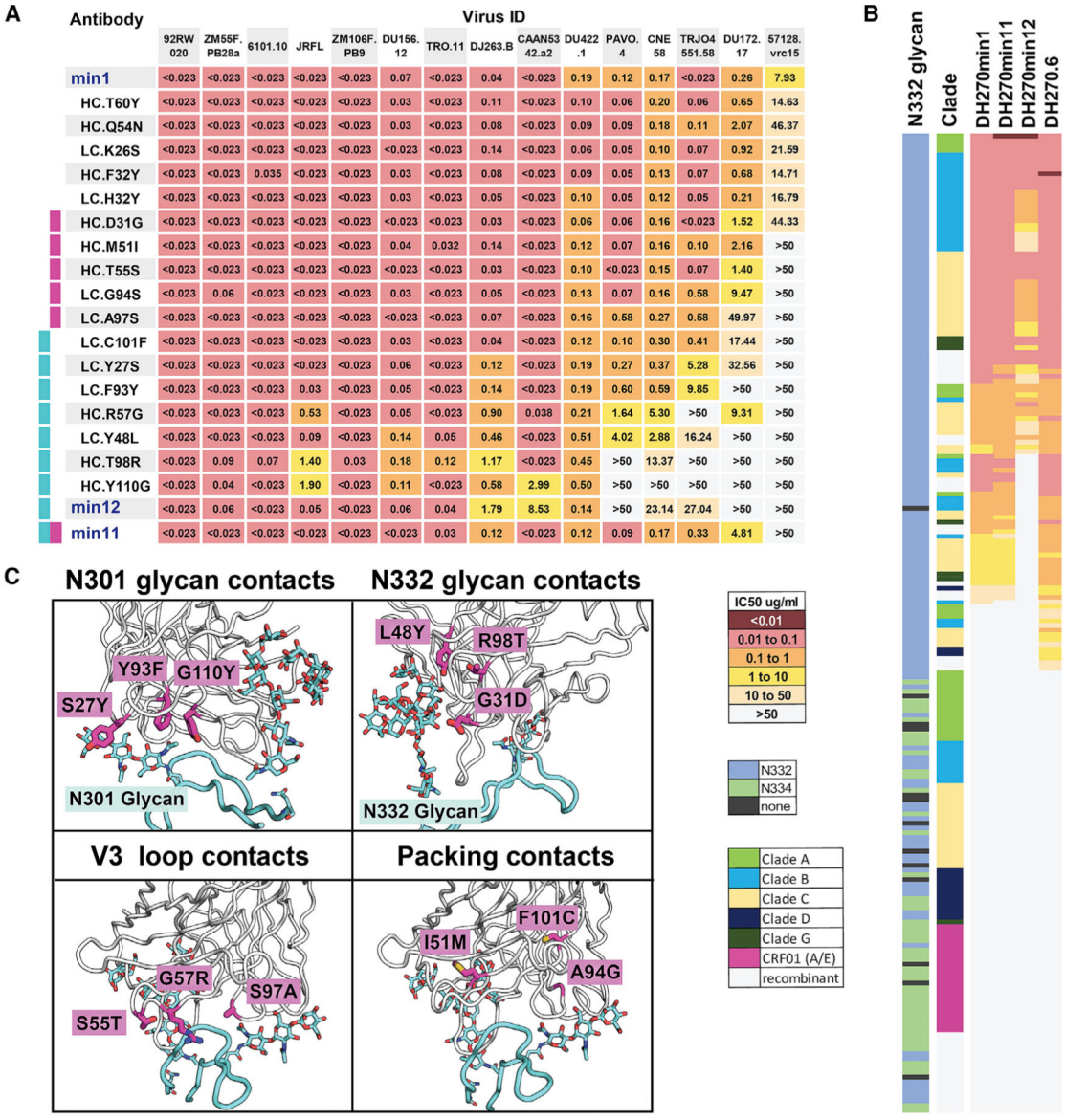

Figure 2. Additional minimization of DH270min1 by single-site mutagenesis

(A) The effect on neutralization of every DH270min1 acquired mutation assessed by single-site mutagenesis to the corresponding UCA residue. Second-generation minimized antibodies DH270min11 and DH270min12 contained only the acquired mutations important for DH270min1 neutralization.

(B) Neutralization breadth of DH270min antibodies on a global panel of 208 pseudoviruses.

(C) Location and binding interactions of the DH270.6 acquired mutations (magenta, sticks) maintained in DH270min11.

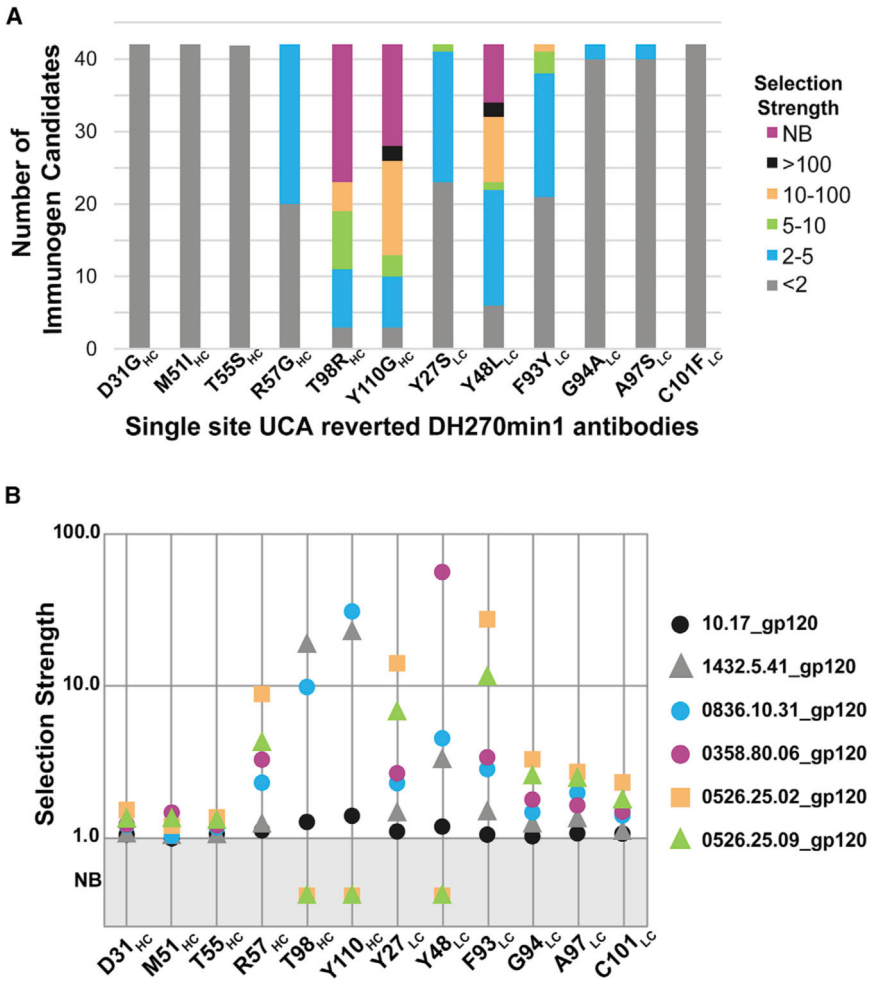

Figure 3. Identification of immunogen candidates that preferentially interact with DH270min1 through its acquired mutations

(A) The number of tested gp120 immunogen candidates that preferentially interact with each of the acquired mutations in DH270min1. Only the acquired mutations present in DH270min11 are displayed. The best 42 gp120 molecules by total DH270min1 affinity are shown.

(B) The selection strength of individual candidate immunogens for each of the acquired mutations present in DH270min11, calculated as the ratio of the binding signal to DH270min1 (logAUC) divided by the binding response (logAUC) to the respective single-site mutated DH270min1 variant. NB, not binding.

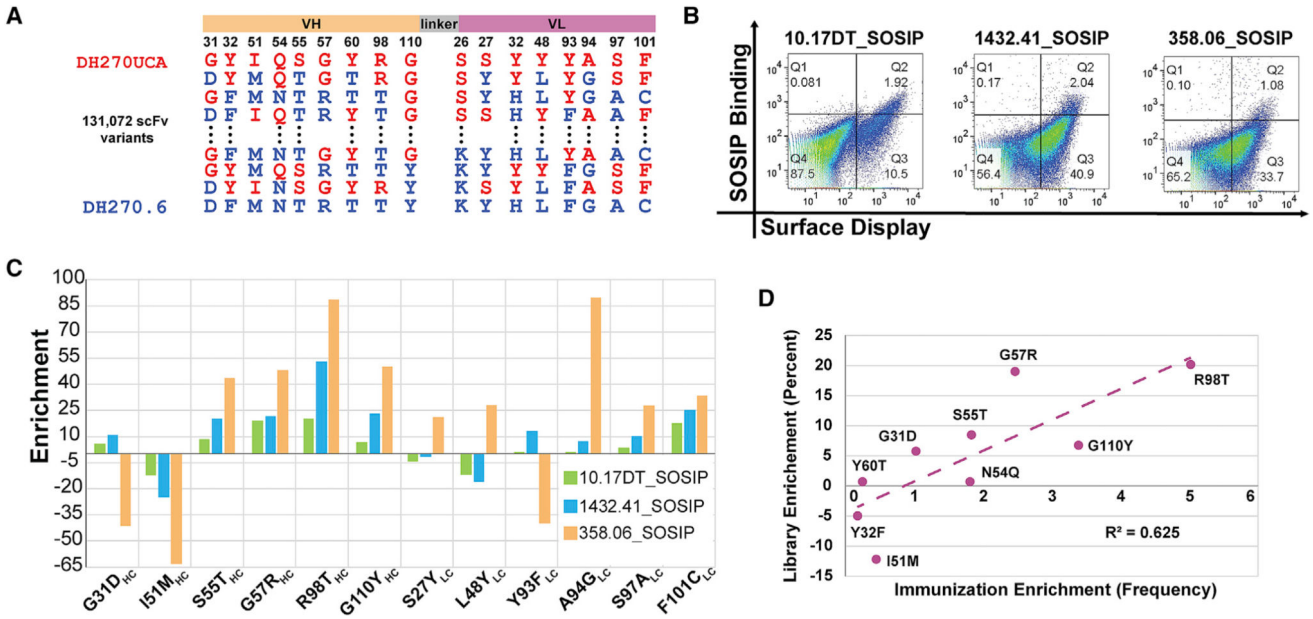

Figure 4. *In vitro* characterization of candidate immunogens toward selection of DH270.6-derived antibodies that contain the acquired mutations present in DH270min1

(A) Design of a scFv library that sampled combinations of acquired mutations present in DH270min1. At each sampled position the amino acid present in the mature DH270.6 monoclonal antibody (mAb) (blue) or that found in the UCA (red) was randomly assorted. (B) Selection of the scFv library for binding to different candidate immunogens by FACS. (C) Enrichment levels of the acquired mutations in the clones isolated by the different immunogen candidates in (B), computed relative to the frequency of the mutations in the unsorted library. Only the key acquired mutations present in DH270min11 are shown. (D) The enrichment of mutations by vaccination, averaged from five DH270UCA knock in mice immunized with 10.17DT (x axis), was plotted against the enrichment of the same mutations in library clones selected by 10.17DT from (C) (y axis). Data were fit with a linear equation ($R^2 = 0.625$). Immunization enrichment was determined by calculating the ratio between the frequency of the observed mutations in the antibody repertoire of vaccinated animals analyzed by next-generation sequencing, and the expected frequency of the mutations in the absence of immunogen selection predicted with ARMADiLLO (Wiehe et al., 2018).

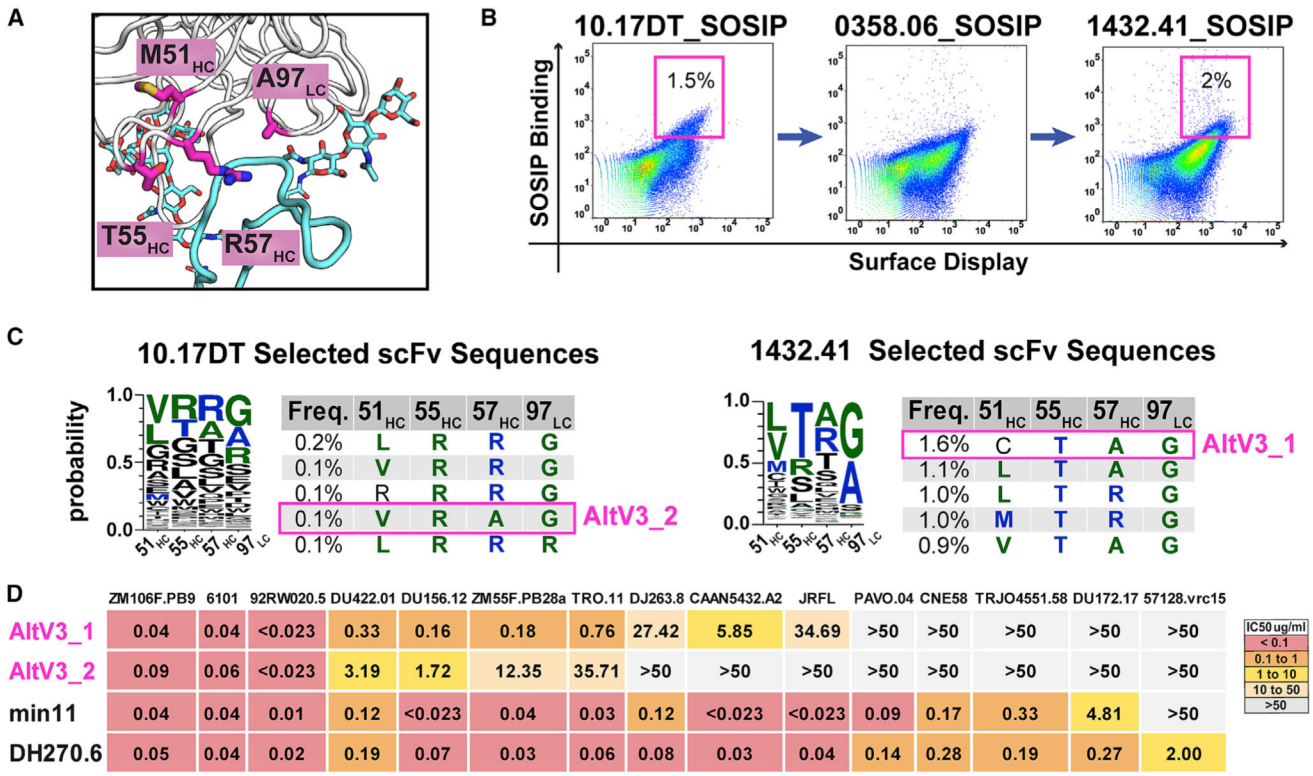

D

	ZM106F.PB9	6101	92RW020.5	DU422.01	DU156.12	ZM55F.PB28a	TRO.11	DJ263.8	CAAN5432.A2	JRFL	PAVO.04	CNE58	TRJO4551.58	DU172.17	57128.vrc15
AltV3_1	0.04	0.04	<0.023	0.33	0.16	0.18	0.76	27.42	5.85	34.69	>50	>50	>50	>50	>50
AltV3_2	0.09	0.06	<0.023	3.19	1.72	12.35	35.71	>50	>50	>50	>50	>50	>50	>50	>50
min11	0.04	0.04	0.01	0.12	<0.023	0.04	0.03	0.12	<0.023	<0.023	0.09	0.17	0.33	4.81	>50
DH270.6	0.05	0.04	0.02	0.19	0.07	0.03	0.06	0.08	0.03	0.04	0.14	0.28	0.19	0.27	2.00

IC50 ug/ml: < 0.1; 0.1 to 1; 1 to 10; 10 to 50; >50

Figure 5. Identification of alternative, more probable amino acids at the DH270min11 acquired mutation sites that contact the Env V3 loop

(A) DH270min11 acquired mutations (magenta, sticks) that interact with the V3 loop (cyan, glycans shown in sticks) ("PDB: 6cbp").

(B) FACS analysis of the scFv library that contains all possible amino acid combinations at the min11 sites in (A), for serial binding to three different SOSIPs. Sequences of the clones sorted in the displayed gates (magenta) were analyzed by PacBio.

(C) Sequence analysis of the clones selected in (B). The DH270.6 amino acid is shown in blue, while mutations more probable than those native to DH270.6 are marked in green. Sequence tables show the frequency of the five most common DH270min11 variants selected by 10.17DT (left) and 1432.41 (right) SOSIP.

(D) Neutralization profile of two selected min11 variants, AltV3_1 and AltV3_2, on a panel of 15 DH270.6-sensitive pseudoviruses.

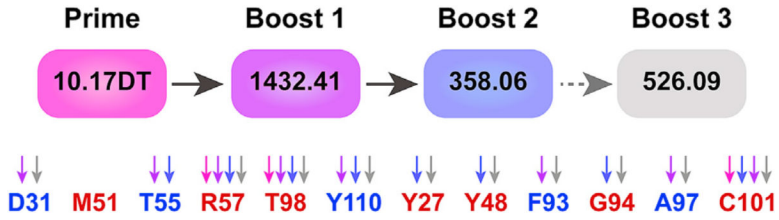

Figure 6. Proposed vaccination regimen for the elicitation of DH270.6-like antibodies that contain the key functional mutations

Priming with the germline targeting immunogen 10.17DT will be followed by successive boosts with molecules identified in this study, 1432.41 and 80.06. If necessary, a final boost with a harder to bind Env, such as 526.09, will be done in order to further expand elicited antibodies with the broadest breadth. Arrows point to the DH270min11 acquired mutations predicted to be selected by the immunogen depicted in the same color. Mutations are colored by probability (red indicates improbable; blue indicates probable).

KEY RESOURCES TABLE

REAGENT or RESOURCE	SOURCE	IDENTIFIER
Antibodies		
DH270.6	Bonsignori et al., 2017a	N/A
DH270UCA3	Bonsignori et al., 2017a	N/A
DH270min1	This paper	N/A
DH270min2	This paper	N/A
DH270min3	This paper	N/A
DH270Prob	This paper	N/A
DH270Improb	This paper	N/A
DH270min11	This paper	N/A
DH270min12	This paper	N/A
DH270min1.G31D.HC	This paper	N/A
DH270min1.M51I.HC	This paper	N/A
DH270min1.T55S.HC	This paper	N/A
DH270min1.R57G.HC	This paper	N/A
DH270min1.T98R.HC	This paper	N/A
DH270min1.Y110G.HC	This paper	N/A
DH270min1.S27Y.LC	This paper	N/A
DH270min1.Y48L.LC	This paper	N/A
DH270min1.F93Y.LC	This paper	N/A
DH270min1.G94A.LC	This paper	N/A
DH270min1.A97S.LC	This paper	N/A
DH270min1.C101F.LC	This paper	N/A
AltMinV3_1	This paper	N/A
AltMinV3_2	This paper	N/A
Chicken anti-c-Myc Antibody- FITC Conjugated	ICL	Cat# CMYC-45F
Goat Anti-Human IgG (γ-chain specific)–R-Phycoerythrin	Sigma-Aldrich	Cat# P9170-.5M; RRID: AB_261239
Streptavidin-R-Phycoerythrin	Sigma-Aldrich	Cat# 42250-1ML
Goat Anti-Human IgG, Fcγ fragment specific-HRP	Jackson Immunoresearch	Cat# 109-035-098; RRID: AB_2337586
Bacterial and virus strains		
see Figure S3		N/A
Chemicals, peptides, and recombinant proteins		
Expi293 media	Thermo Fisher	Cat# A1435101
Optimem	Invitrogen	Cat# 31985088
Expifectamine	Thermo Fisher	Cat# A14524
Protein A Beads	Thermo Fisher	Cat# PI-20334
Pen-Strep	Sigma-Aldrich	Cat# P4333-100ML
Kanamycin	VWR	Cat# 10128-224

REAGENT or RESOURCE	SOURCE	IDENTIFIER
Q5 Master Mix	NEB	Cat# M0494S
MiSeq Reagent Kit v3	Illumina	Cat # MS-102-3001
QIAquick Gel Extraction Kit	QIAGEN	Cat # 28706X4
High Fidelity Phusion Polymerase	NEB	Cat # E055S3
QIAquick PCR and Gel Cleanup Kit	QIAGEN	Cat # 28506
Bam-HI restriction enzyme	NEB	Cat # R3136M
SalI-HF restriction enzyme	NEB	Cat # R3138M
NheI-HF restriction enzyme	NEB	Cat # R3131M
SDCAA media	Teknova	Cat # 2S0540-06
SGCAA media	Teknova	Cat # 2S0542-02
Zymoprep Yeast Plasmid Miniprep Kit	Zymo Research	Cat # 76212-310
Wizard Plus SV Minipreps	Promega	Cat # A9282
293fectin	Thermo Fisher	Cat# 12347019
Ni-NTA Agarose	QIAGEN	Cat # 30230
TMB Substrate	KPL	Cat# 53-00-03
Deposited data		
Crystal structure of DH270.6 scFv in complex with Man9-V3 glycopeptide	Fera et al., 2018	PDB: 6CBP
Experimental models: Cell lines		
E. coli NEB 5α strain	NEB	Cat# C2987H
Human cell line Expi293F	Thermo Fisher	Cat #14527
S. cerevisiae EBY100 strain	ATCC	Cat# MYA-4941
Human cell line TZM-bl	NIH ARRRP	Cat #8129
Human cell line FreeStyle 293F	Thermo Fisher	Cat #R790-07
Oligonucleotides		
yeast_lib_sequencing: CAGATCTCGAGCTATTACAAGTC	This paper	N/A
yeast_lib_NGS: TCTGCAGGCTAGTGGTG; CAAGTCCTCTTCAGAAATAAGC	This paper	N/A
Recombinant DNA		
pCTcon2	Chao et. al., 2006	Addgene Cat# 41843
Software and algorithms		
PyMOL Version 2.4.0	Schrodinger, LLC	https://pymol.org/2/
Geneious Version 2021.1.1	Biomatters	https://www.geneious.com/prime/
Rosetta	RosettaCommons	https://www.rosettacommons.org/software/license-and-download
Rosetta REF2015	Park et al., 2016	N/A
Rosetta Backrub	Lauck et al., 2010	rosetta/main/source/src/apps/public/backrub.cc

REAGENT or RESOURCE	SOURCE	IDENTIFIER
FlowJo Version 10.7.1	BD	https://www.flowjo.com/solutions/flowjo/downloads
SoftMax Pro Version 5.3	Molecular Devices	https://www.moleculardevices.com/products/microplate-readers/acquisition-and-analysis-software/softmax-pro-software#gref
Excel	Microsoft	https://www.microsoft.com/en-us/microsoft-365/excel
PISA	Krissinel and Henrick, 2007	https://www.ebi.ac.uk/pdbe/pisa/
WebLogo 3	Crooks et al., 2004	https://github.com/WebLogo/weblogo/